

## Article

# Improving Wear Resistance of Highly Porous Titanium by Surface Engineering Methods

Serhii Lavrys <sup>1,\*</sup>, Iryna Pohrelyuk <sup>1</sup>, Juozas Padgurskas <sup>2</sup> and Khrystyna Shliakhetka <sup>3</sup>

<sup>1</sup> Department of Material Science Bases of Surface Engineering, Karpenko Physico-Mechanical Institute of the NAS of Ukraine, 79060 Lviv, Ukraine; irynapohrelyuk@gmail.com

<sup>2</sup> Department of Mechanical, Energy and Biotechnology Engineering, Vytautas Magnus University, 44248 Kaunas, Lithuania; juozas.padgurskas@vdu.lt

<sup>3</sup> Institute of Materials and Machine Mechanics, 84511 Bratislava, Slovakia; khshvachko@gmail.com

\* Correspondence: lavrys92@gmail.com; Tel.: +380-938421426

**Abstract:** The wear resistance of highly porous titanium in the tribo-pair with bronze under boundary lubrication condition was investigated. According to analyses of worn surfaces of highly porous titanium, it was shown that the main reason of poor wear resistance were subsurface pores that led to nucleation of micro-cracks in the subsurface layer and thereby intensified fatigue (delamination) wear. For improvement of wear resistance of highly porous titanium, the surface engineering methods, such as deformation (ball burnishing, BB), diffusion (gas nitriding, GN), and their combination—deformation–diffusion treatment (DDT), were considered. It was shown that surface hardening of highly porous titanium by BB, GN, and DDT reduces the weight wear intensity and the friction coefficient of the tribo-pairs by 1.4, 3.5, 4.0 and 1.8, 2.3, 3.2 times, respectively. Such an improvement in the tribological properties of highly porous titanium after surface hardening is explained by changes in the main wear mechanism of the tribo-pairs from adhesive and fatigue to abrasive. The highest wear resistance of highly porous titanium was observed after surface deformation–diffusion treatment, as this treatment provides a combination of the positive effects of both ball burnishing (closing of surface pores) and nitriding (formation of a surface chemically inert and hard nitride layer).

**Keywords:** powder metallurgy; titanium; porosity; surface engineering; friction; wear mechanism; wear resistance



**Citation:** Lavrys, S.; Pohrelyuk, I.; Padgurskas, J.; Shliakhetka, K. Improving Wear Resistance of Highly Porous Titanium by Surface Engineering Methods. *Coatings* **2023**, *13*, 1714. <https://doi.org/10.3390/coatings13101714>

Academic Editor: Jinyang Xu

Received: 30 August 2023

Revised: 21 September 2023

Accepted: 27 September 2023

Published: 29 September 2023



**Copyright:** © 2023 by the authors. Licensee MDPI, Basel, Switzerland. This article is an open access article distributed under the terms and conditions of the Creative Commons Attribution (CC BY) license (<https://creativecommons.org/licenses/by/4.0/>).

## 1. Introduction

Titanium has at least three unique properties: high specific strength, excellent corrosion resistance in many corrosive media and biocompatibility. Therefore, titanium is an ideal material for almost all sectors of the industry. However, the manufacturing of titanium mainly depends on the needs of aerospace and medical applications, which is explained by the high-cost manufacturing. It is several times higher than the manufacturing of steel or aluminum. That is, only for the aerospace industry and medicine the unique and practically irreplaceable properties of titanium are more important than its price. The high cost of titanium production is due to the complex traditional technology, which includes the process of multiple vacuum remelting, thermo-mechanical processing, forging and subsequent rough machining. Using this technology, in order to achieve the final dimensions of the part, approximately 20%–90% of the wrought titanium is removed [1–6]. Powder metallurgy (PM) is one of the perspective directions to solve this problem. PM reduces rough machining costs and increases material yield. This technology makes it possible to produce parts with complex geometry and products with dimensions close to final ones [4–11].

However, titanium obtained by the PM method has one characteristic structural feature—residual porosity. Usually, the porosity of titanium is a structural defect that negatively influences the mechanical, fatigue, anti-corrosion and other characteristics of

titanium [12–26]. For example, an increase in porosity reduces the corrosion resistance of titanium, since surface pores increase the contact area of contact with an aggressive medium [12–14]. In addition, with an increase in porosity, the fatigue characteristics of titanium decrease, since pores (especially surface ones) initiate the nucleation and growth of fatigue cracks, which ultimately leads to fracture [15–17].

However, it should be noted that, according to literature sources, non-porous deformable titanium has low tribological characteristics, which makes it impossible to use it in tribo-pairs without additional surface engineering [27–30]. The poor wear resistance of titanium is due to a number of its properties such as low thermal conductivity, high chemical activity, and low hardness. Therefore, it is logical that porous titanium also needs additional surface engineering, but taking into account its structural feature—porosity.

Unfortunately, the effect of porosity on the tribological characteristics of titanium is still poorly understood. This can be explained by the fact that tribology is a system response and not a property of a material. That is, tribological characteristics depend not only on physico-mechanical properties of the material but also on the friction conditions (temperature, environment, lubrication type etc.) and on the properties of the counterbody material. Therefore, porosity can have both a negative and a positive effect on the tribological properties of titanium. For example, works [18–20] show that porosity negatively affects tribological characteristics because surface pores decrease the real contact area between the frictional (sliding) surfaces that increases the contact pressure and stress on the surface and, as a result, intensifies the wear rate. In addition, surface pores can act as concentrators and places of cracks nucleation and propagation in the near-surface layers during friction, which increases the fatigue wear (delamination) of titanium. Liu et al. [21] determined that the edges of the surface pores act as ‘cutters’ which intensify the abrasive wear of the counterbody and increase the probability of rupture and chipping of the edge of the pores and the development of three-body abrasive wear. On the other hand, under boundary lubrication, pores can act as reservoirs for body fluids and may improve anti-friction properties and wear resistance of a tribo-pair [22–24]. Munagala et al. [25] investigated pores in Ti6Al4V coating that captured the wear debris and decreased its wear due to the abrasion. Chen et al. [26] showed that porosity is not always detrimental. The small amount of pores under some conditions appears to be useful to the erosion resistance of the composite. They suggested that porosity might help absorb impact energy that accompanies crack splitting, which reduces crack propagation and delays rapid fracture. Therefore, when evaluating effect of porosity on the tribological characteristics, it is necessary to take into account the operating conditions of a tribo-pair, that is, the scope of application of porous titanium.

Given the fact that PM titanium has the same high specific strength and corrosion resistance and at the same time is cheaper than wrought titanium, it is promising material for vehicle engineering. For example, it can be used to make components of bearings, engines, and hydraulic cylinders of cars operating under boundary lubrication conditions in tribo-pair with bronze. Parts made of titanium allow both the enhancement of the resource and the reduction in the weight of the vehicle and, as a result, reduction in energy costs for maintenance [27,31–36].

Based on this, the aim of this work is to investigate wear mechanisms of porous titanium under boundary lubrication conditions and to propose methods of surface engineering for improving its wear resistance.

## 2. Materials and Methods

### 2.1. Material Manufacturing

Porous titanium manufactured by powder metallurgy were investigated. As starting (raw) powder, titanium hydride  $TiH_2$  powder was used, obtained from Joint-Stock Company Titanium Institute (Zaporizhzhia, Ukraine). Before vacuum sintering, titanium hydride  $TiH_2$  was ground in a RETSCH PM100 planetary mill (powder mixture fractions did not exceed

40  $\mu\text{m}$ ) and pressed at a specific load of 400 MPa by a P-125 hydraulic press at 20  $^{\circ}\text{C}$ . Sintering was carried out using the SNVE-1.3.1 electric furnace in a vacuum (13 Pa) at 1100  $^{\circ}\text{C}$  for 4 h with subsequent furnace cooling. The cylindrical samples (Figure 1) were cut from the obtained rectangular billets. The samples were polished to the surface roughness of  $R_a = 0.2 \mu\text{m}$ . The porosity of the obtained titanium samples determined by Archimedes' method was 20%.

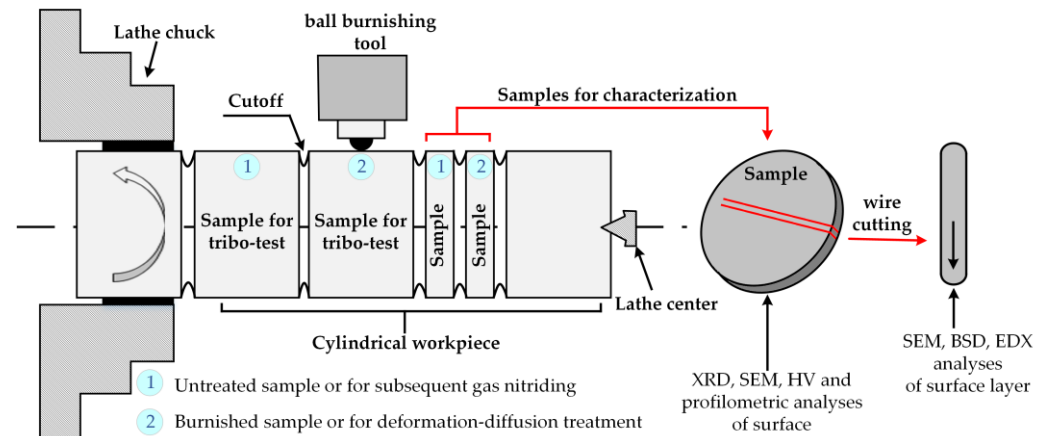


**Figure 1.** Scheme of sample preparation for characterization.

## 2.2. Surface Engineering

In this work, we tried to evaluate some methods of surface engineering, which, in our opinion, are promising for the following reasons:

- **Ball burnishing (BB).** Choosing this method can be explained by the fact that the surface plastic deformation of titanium makes it possible, due to the refinement of grains and an increase in linear and point defects in the near-surface layer, to increase the hardness and as a result improve the wear resistance of titanium [30,37–40]. Also, plastic deformation ensures the formation of a compacted surface layer, that is, it contributes to the closing of pores [41,42]. Such closing of the near-surface pores makes it possible to less the negative effect of porosity during friction because this leads to a decrease in places of cracks nucleation and propagation. In this case, BB was carried out using a 1K62 universal screw-cutting lathe at room temperature. A ball with a diameter of 5 mm is made of diamond polycrystalline composite material  $C_d-Co-34Ni$  [31]. Lubrication type—boundary lubrication in an industrial oil I-20A. BB regime: load—100 N; speed—200 rpm; the number of passes—3. A ball with a diameter of 5 mm is made of a diamond polycrystalline composite material [27].
- **Gas nitriding (GN).** This method is chosen taking into account that the formation of a surface chemically inert nitride compound layer with high hardness significantly improves the wear resistance of titanium [43–47]. The formed protective nitride compound layer also partially closes (covers) the surface pores, which perhaps reduces their negative effect on wear resistance of titanium. GN is carried out using equipment developed by Karpenko Physico-Mechanical Institute of NAS of Ukraine. GN regime: heating up to a temperature of 750  $^{\circ}\text{C}$ , exposure for 5 h; subsequent heating at a rate of 5  $^{\circ}\text{C} \times \text{min}^{-1}$  to a temperature of 800  $^{\circ}\text{C}$ ; cooling with a furnace. For GN, commercially pure gaseous nitrogen is used.
- **Deformation–Diffusion treatment (DDT).** This treatment is based on a combination of preliminary surface plastic deformation and subsequent thermochemical treatment. This combination is used due to the fact that as a result of preliminary plastic deformation, phase redistribution processes occur in the surface layer, residual compressive stress, the area of grain boundaries, the density of dislocations and point defects, which are favourable channels for facilitated diffusion of nitrogen, is increased. This makes it possible to form layers (in our case, nitride layers) with higher wear resistance and

hardness compared to conventional gas nitriding [27,48–50]. Combined DDT includes preliminary BB and subsequent GN of titanium, according to the above-mentioned BB and GN regimes.

### 2.3. Material Characterization

The phase-structural state of samples was determined by XRD analysis using a DRON-3.0 diffractometer (Burevestnik, Nizhny Novgorod, Russia) in Cu K $\alpha$  radiation. The anode voltage was 30 kV, and the current was 25 mA. Diffraction patterns were registered in the  $2\theta$  angle range—10 . . . 90°. Scan step was 0.05°, exposure time—5 s. The surface roughness (parameter Ra) was measured by a 170,621 profilometer (Standart Pribor, Kyiv, Ukraine). Durometric analysis was carried out by means of a PMT-3M microhardness tester (Lomo, St. Petersburg, Russia) at a load of 0.49 N on the Vickers indenter. The surface topography and microstructure were investigated by the EVO 40XVP scanning electron microscope (SEM) (Carl Zeiss, Oberkochen, Germany) equipped with a backscattered electron detector (BSD) and INCA Energy dispersive X-ray (EDX) microanalysis (Oxford Instruments, Abingdon, UK). The porosity of the near-surface layer was determined using the ImageJ software (Version 1.8.0). The scheme of the sample preparation for the characterization is presented in Figure 1.

### 2.4. Tribological Test

The tribological characteristics were studied using an SMT-2 friction machine (Tochpribor-KB, Russia) with automatic registration of coefficient of friction (COF) and temperature near the friction zone (TOF) at a specific load of 1 MPa. The friction exposure and rate were 3000 s and 0.6 m  $\times$  s<sup>-1</sup>, respectively. Friction scheme—‘disk–block’ (Figure 2). Friction was carried out under boundary lubrication in industrial oil I-40 (GOST 20799-88). Disks (bodies) were made of porous titanium in the initial state and after surface treatments. The blocks (counterbodies) were made of bronze (Cu-10Al-4Ni-4Fe). The surface roughness Ra of the counterbody was 0.2  $\mu$ m. The chemical composition and mechanical characteristics of the bronze counterbody are shown in Table 1. Tribological tests were performed at 20 °C. The TOF was determined using a chromel–alumel thermocouple, which was fixed to the counterbody (Figure 2). Such friction conditions and the material of counterbody were chosen in view of previous studies, where the prospect of using titanium and its alloys as a structural material in hydraulic systems was considered [27,39]. The wear resistance of the studied tribo-pairs was evaluated by their weight change after friction. Weighing of the specimens after friction was determined by VP64C analytical balance (OHAUS, Parsippany, NJ, USA) with the accuracy of  $\pm$ 1 mg. Before and after tribological tests, the samples were washed in gasoline, acetone, alcohol and thermal dried in a vacuum furnace at a temperature of 200 °C. This procedure was performed to remove residual liquid and oil from surface pores. For evaluation of each surface engineering method, at least three tribo-pairs were tested to ensure reproducibility.

**Table 1.** Chemical composition and mechanical characteristics of Cu10Al4Ni4Fe bronze (GOST 18175-78).

Chemical Composition, wt. %											
Element	Al	Fe	Ni	Mn	Zn	Sn	Si	Pb	P	Others	Cu
max	9.5	3.5	3.5	0.3	0.3	0.1	0.1	0.02	0.01	0.6	Balance
min	11.0	5.5	5.5	–	–	–	–	–	–	–	–
Mechanical properties											
Ultimate tensile strength, MPa									640		
Elongation, %									5		
Vickers microhardness, GPa									1.5 $\pm$ 0.1		

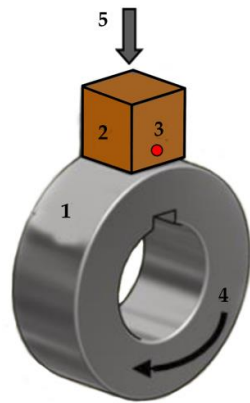


**Figure 2.** Friction scheme of «disk–block»: 1—titanium disk (body), 2—bronze block (counterbody), 3—hole for thermocouple, 4—rotational direction, 5—normal load.

### 3. Results

#### 3.1. Surface Characteristics

After BB, the surface microhardness of titanium increases by approximately twofold (Figure 3a). Due to the smoothing of surface microrelief (Figure 4b), the roughness is improved twofold compared to the initial one (Figure 3b). The microstructural analysis shows that due to local plastic deformation, the pores in near-surface layer of titanium are closed (healed). That is, a consolidated surface layer with a thickness of 200 μm and a porosity of about 1% is formed (Figure 5b).

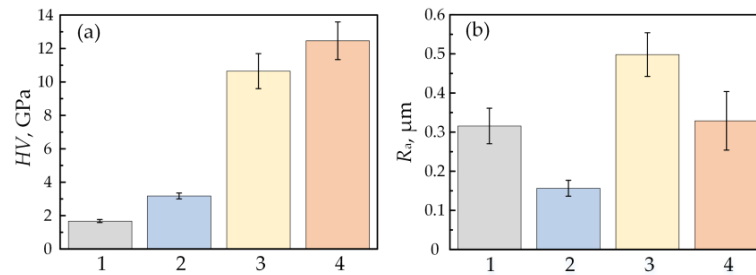


**Figure 3.** Surface microhardness (a) and roughness (b) of highly porous titanium in initial state (1) and after BB (2), GN (3), DDT (4).

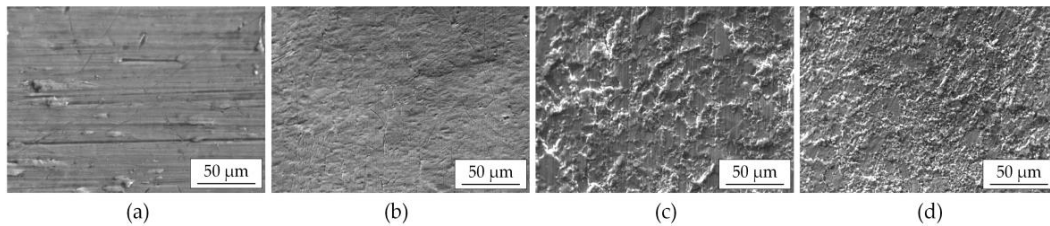


**Figure 4.** Surface topography of highly porous titanium in initial state (a) and after BB (b), GN (c), DDT (d).

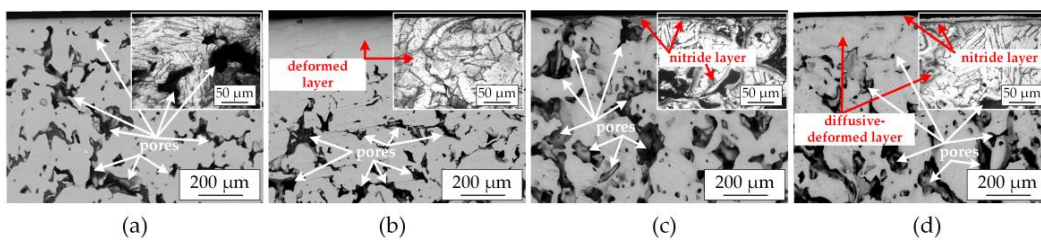


**Figure 5.** Scanning electron backscattering morphologies of cross-section of highly porous titanium in initial state (a) and after BB (b), GN (c), DDT (d).

The surface microhardness of the titanium increases by four times (Figure 3a) due to the formation of the compound nitride layer after GN (Figure 5b). However, the surface roughness deteriorates by 1.6 times (Figure 3b) since a characteristic surface microrelief is formed, and it reproduces grain boundaries of titanium (Figure 4c). It can be caused by the increased intensity of penetration of the atoms through the grain boundaries, as they are favourable paths for their facilitated diffusion [43]. The porosity in the near-surface layer increases from 20 to 25%, and the pore size also increases (Figure 5c). Such an increasing porosity can be explained by the formation of a nitride compound layer on the pore surface which expands subsurface pores due to the density difference between titaniums (TiN density— $5.4 \text{ g/cm}^{-3}$  vs.  $\alpha$ -Ti density— $4.5 \text{ g/cm}^{-3}$ ).

After DTT, an increase in the surface microhardness by 4.6 times is observed (Figure 3a). Higher level of surface microhardness after DDT than after GN is explained by the intensification of nitride formation processes, which is confirmed by higher reflections of nitride phases in the diffraction patterns (Figure 6). That is, as a result of preliminary plastic deformation, phase redistribution processes occur in the surface layer; residual compressive stress, the area of grain boundaries, the density of dislocations and point defects, which are favorable channels for facilitated nitrogen diffusion, are increased. Surface roughness deteriorates, but it is better than after nitriding (Figure 3b). It is that preliminary BB due to surface smoothing that makes it possible to form a less relieving topography of the nitrided surface (Figure 4d). Also in the near-surface layer, a slight increase in porosity, not exceeding 5%, is observed (Figure 5d).

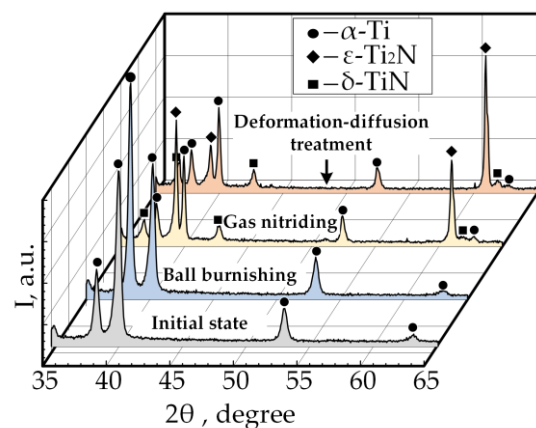


**Figure 6.** Diffraction patterns registered from highly porous titanium surface in initial state and after surface engineering.

### 3.2. Tribological Characteristics

Analysis of the kinetics of COF changes (Figure 7a) showed that at the initial stage of the test, the friction coefficient for all tribo-pairs decreased and stabilized. Analysis of the kinetics of COF changes (Figure 7a) showed that COF of tribo-pair where porous titanium in its initial state was unstable throughout the studied period. Also, for untreated porous titanium, a high amplitude of COF oscillations was observed, which is evidence of intensive frictional processes (Figure 7a). But for surface-treated porous titanium, the COF after 500 s decreased and stabilized, which means that the tribo-surfaces of the tribo-pairs were running. Surface hardening of porous titanium by the BB, GN, and DDT methods made it possible to reduce the COF of the studied tribo-pairs by 1.8, 2.3, and 3.2 times, respectively. The character of the curves of TOF changes correlated well with COF (Figure 7). Therefore, for a tribo-pair, where untreated porous titanium was used, the highest temperature in the friction zone was recorded. It indicated the highest intensity of plastic deformation and diffusion processes in the surface layer. The lowest COF and TOF values were recorded for a tribo-pair, where titanium hardened by DDT.

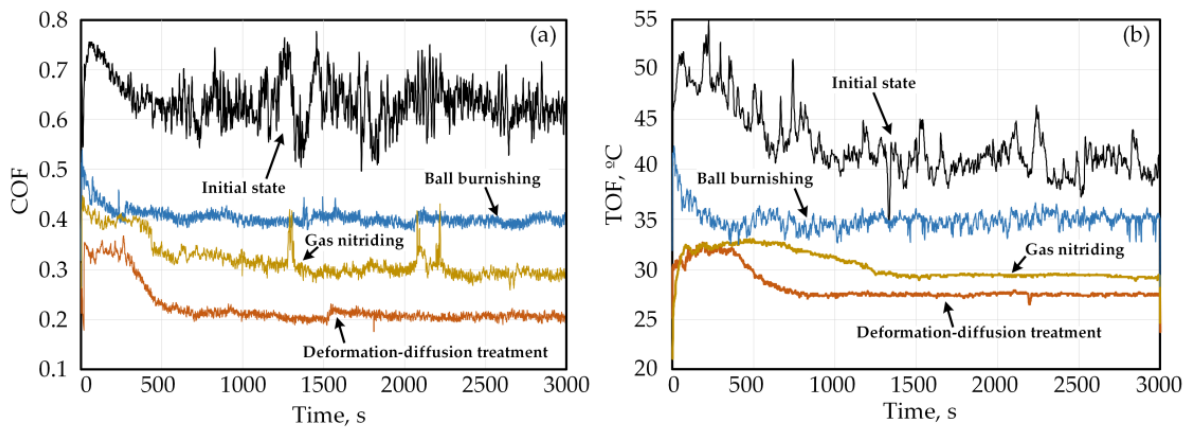


**Figure 7.** Kinetics changes in COF (a) and TOF (b) for tribo-pairs ‘highly porous titanium—bronze’.

It was found that the wear intensity of the counterbody (bronze) was higher than that of porous titanium, regardless of the surface treatment (Figure 8). Surface hardening of highly porous titanium by BB, GN, and DDT methods allowed reduction in the wear intensity of the counterbody of 1.5, 3.6 and 3.9 times, respectively. However, we did not observe a similar dependence of the wear intensity for the body (porous titanium). In particular, untreated and surface-hardened by BB porous titanium after friction lost its weight, which indicated its wear. The weight of porous titanium hardened by GN and DDT increased after friction, which indicated the transfer of bronze to the titanium surface. Thus, GN and DDT of porous titanium provided the highest wear resistance under such tribo-interaction conditions (Figure 8).

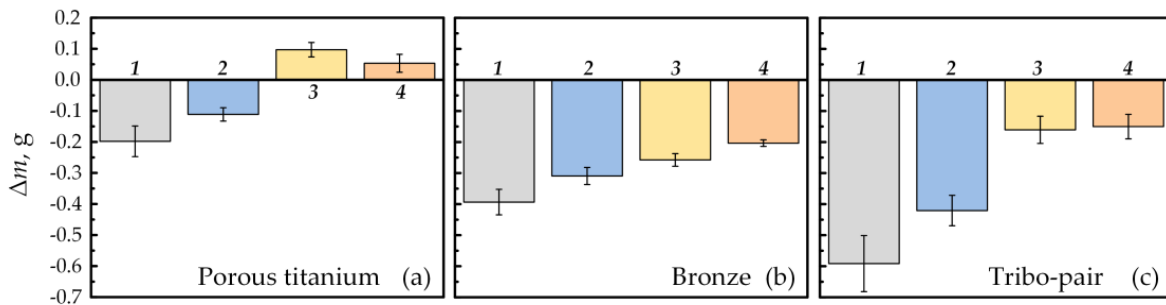


**Figure 8.** Weight change in titanium body (a), bronze counterbody (b) and tribo-pair (c), where highly porous titanium in initial state (1) and after BB (2), GN (3), DDT (4).

#### 4. Discussion

In this research, to explain the tribological behavior of porous titanium, the wear mechanisms of friction pairs were investigated. An analysis of the topography of the wear surfaces of porous titanium and bronze shows that friction of tribo-pairs lead to wear by several mechanisms: adhesive (junction), fatigue (delamination), abrasive and oxidative. On the worn surface, the characteristic peculiarities of these mechanisms were observed: smearing areas (transferred materials) and craters corresponding to adhesive mechanism; delamination areas of subsurface layer and micro-cracks—fatigue mechanism; areas of grooved relief—abrasive mechanism; areas with increased oxygen content on the surface—oxidative mechanism (Figures 9–11 and Table 2).

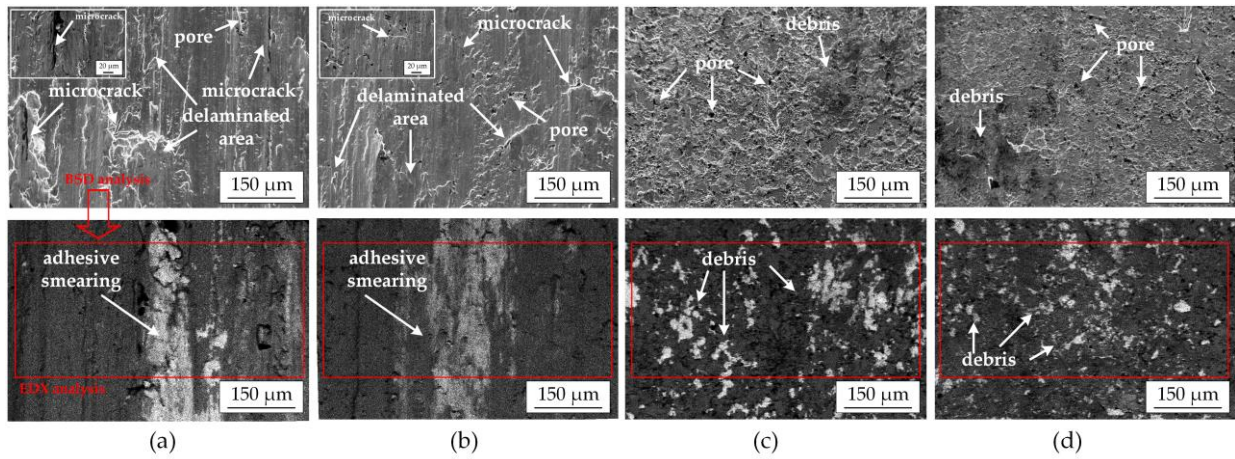


**Figure 9.** SEM images with DSD (below) and EDX (red selection) analysis of highly porous titanium (body) worn surface: titanium in initial state (a) and after BB (b), GN (c), DDT (d).

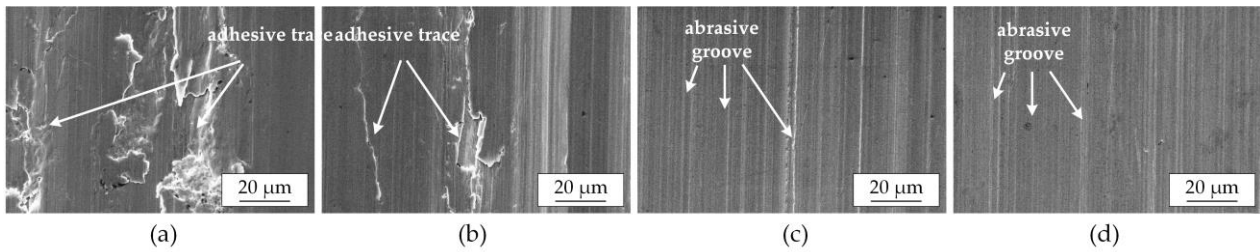


**Figure 10.** SEM images of bronze (counterbody) worn surface after friction with highly porous titanium in initial state (a) and after BB (b), GN (c), DDT (d).

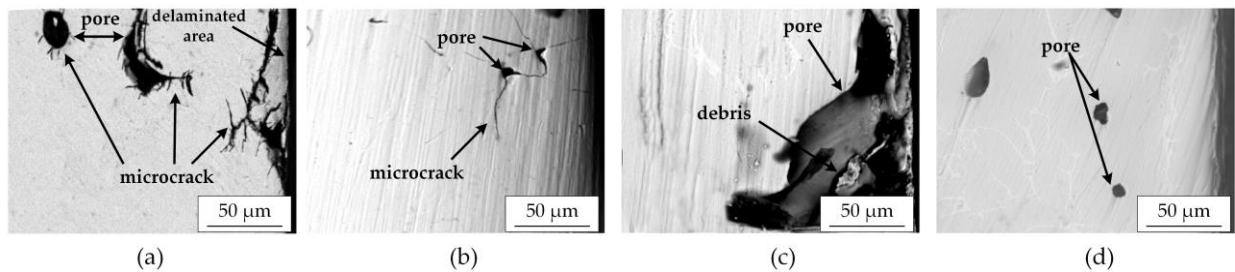


**Figure 11.** Scanning electron backscattering morphologies of cross-section of worn subsurface, cross-sections parallel to sliding direction of c. p. titanium in initial state (a) and after BB (b), GN (c), DDT (d).

**Table 2.** EDX analysis of worn surfaces of highly porous titanium after friction with bronze (see Figure 9).

Analysis	Element Content, wt. %/at. %						
	Ti	N	Cu	Al	Fe	Ni	O
Figure 9a	41.94/39.71	-/-	29.62/20.37	8.42/9.93	0.73/0.35	0.55/0.51	18.81/29.13
Figure 9b	53.01/52.36	-/-	26.93/18.40	7.32/7.01	0.34/0.21	0.95/0.90	11.45/21.12
Figure 9c	47.71/45.87	6.52/14.98	35.68/24.77	3.96/7.76	3.18/3.14	0.89/0.59	2.06/2.89
Figure 9d	67.11/54.48	13.51/29.39	15.03/12.22	1.80/1.88	1.02/0.56	0.35/0.18	1.18/1.29

The main (dominant) are the adhesive and fatigue wear mechanisms. Their characteristic features prevail on the worn surfaces of porous titanium and bronze. Such wear mechanisms describe the interaction of friction surfaces, accompanied by severe plastic deformation of thin subsurface layers under loads exceeding yield strength of materials. However, the nature of these wears mechanisms is different. Adhesive wear is realized in process of frictional interaction due to destruction of a protective oxide film and baring of the surface of chemically reactive titanium. During friction at an interatomic distance, adhesive junctions of contact surfaces occur with energy release. When the molecular interaction between micro cold-welded surfaces is higher than the tensile strength of contact materials, and bodies continue to move mutually, the softer metal is removed and transferred to another surface. The adhesive craters are formed on the contact surface of metal samples with lower hardness (bronze) (Figure 10a), and adhesive smearing—on samples with higher hardness (titanium) (Figure 9a). It was confirmed by EDX analysis of surfaces after friction (Table 2): bronze (light areas) was observed on the surface of titanium samples (Figure 9a). Such smearing areas are directed with sharp edges towards the sliding direction.

Fatigue wear is realized due to plastic deformation in the contact zone, which contributes to maximum convergence of tribo-surfaces and formation of texture in surface layers from extremely deformed grains located in a direction of the relative frictional movement of tribo-surfaces (Figure 9a). Due to the high cyclic loads during friction, several deformed layers are formed in surface layer of titanium, in which cracks nucleate, unite with each other and propagate to the surface (Figures 9 and 11a). The individual areas of surface layer peel off and separate from the surface; the delamination process occurs (Figure 9a).

It should be noted that subsurface pores, which behave as additional stress concentrators and, consequently, become centres of nucleation of surface cracks, are the cause of the delamination during the friction of porous titanium. Thus, according to the metallographic analysis of the section of porous titanium after friction (Figure 11a), the initiation and propagation of cracks, which occurs not only on the surface of several deformed layers but also in the pores, was observed. That is, plastic deformation is concentrated not only in subsurface layer but also near the pores, from which many cracks begin to grow (Figure 10a). It indicates intensive delamination processes. Therefore, it can be assumed that the porosity of titanium during friction in the tribo-pair with bronze under boundary lubrication conditions is a negative structural factor which intensifies the wear of porous titanium by the fatigue mechanism (delamination). This assumption is confirmed in [38,39], where, with an increase in porosity, the wear resistance of aluminum and its alloys decreased due to an increase in the centres of crack initiation in subsurface pores during friction. Also, in studies [51–53], the positive influence of porosity on the wear resistance of materials is noted (porous iron and composite). This is explained by the fact that during friction under conditions of boundary lubrication, pores act as additional reservoirs for the lubricant, which, under load during friction, is squeezed into the tribo-contact zone and reduces both the friction coefficient and wear intensity. However, in our case, this effect was not observed. This is due to the presence of an adhesive component in the wear of these tribo-pairs, when bronze, smearing to the titanium surface, closes the subsurface pores and, consequently, levels the previously mentioned effect. In addition, it can have a negative effect on the tribological behaviour of titanium in this tribo-pair. Under the influence of applied loads during the friction, the opening and growing of cracks in the pores can also occur due to the pulsating oil pressure in closed pores.

It can be assumed that the oxidative and abrasive wear mechanisms are secondary ones because their appearance is caused by adhesive and fatigue wear. Due to adhesion and fatigue wear during friction, the wear products (transferred materials, delaminated layers, debris, etc.) do not always leave the contact zone, but under the action of high loads and temperatures between two contact surfaces, they can oxidize in situ and form local areas of brittle oxides of contact materials, which subsequently are chipped off. This assumption about the formation of oxides on worn surfaces was confirmed by EDX analysis

(Table 2), which recorded oxygen, the content of which on the surface exceeds the maximum solubility in  $\alpha$ -titanium. Since the oxides have higher hardness (for example, the hardness of  $\text{TiO}_2$  dioxide is several times higher than that of titanium) and chemical inertness (not cold-welded during friction) compared to the contact materials, they provoke abrasive wear by two (if the oxide areas are still fixed to the surface) or three (if the oxide areas are chipped off from surface) body mechanisms. The realization of this mechanism was confirmed by the SEM analysis of worn surfaces of porous titanium and bronze: minor local grooves, scratches, scuffing, etc., which are characteristic signs of the abrasive wear mechanism, were observed. The signs of oxidative wear mechanism were observed on surface of porous titanium, and the signs of abrasive mechanism were mostly fixed on the surface of soft material—bronze. Obviously, in the process of friction, titanium oxides are formed on the surface of titanium, which leads to abrasive wear of softer bronze.

The frictional behaviour of BB porous titanium is similar to that of untreated titanium. That is, the wear of deformation hardened porous titanium in the tribo-pair with bronze occurs according to the same mechanisms: adhesion, fatigue, oxidative and abrasive (Figures 8 and 9b), as in untreated porous titanium. However, the wear rate in the case of deformation hardened surface is lesser, which improves the wear resistance of porous titanium.

It was confirmed by SEM (Figures 8 and 9b) and EDX (Table 2) analyses since there were fewer adhesion areas on the titanium surface (Figure 9b and Table 2) and adhesive craters on the surface of the bronze counterbody (Figure 9b). According to the Archard equation [52,54], the main parameter for adhesive wear is surface hardness. Since the surface plastic deformation during BB provides higher surface microhardness in comparison with untreated titanium (Figure 3a), it leads to an increase in the adhesion resistance of porous titanium under friction conditions. It should also be noted that in a recent study [55], the Archard equation was corrected, where, in addition to hardness, an important role was assigned to surface roughness: the better the surface quality (less surface relief), the higher the wear resistance of the material. In our case, BB reduces the roughness parameter  $R_a$  (Figure 3b) and surface relief (Figure 4b) in comparison with untreated porous titanium; that is, it improves surface quality, increasing adhesive wear resistance of porous titanium.

After BB, the fatigue wears resistance of porous titanium is also improved, which was confirmed by the results of SEM analysis: a smaller number of delamination areas and surface micro-cracks on the worn surface was observed (Figure 8b). As a result of surface deformation, the pores in the surface layer of titanium closed and practically disappeared (Figure 4b). It can be assumed that a decrease in the number and size of subsurface pores reduces the probability of formation of cracks in the subsurface layer and their emergence on the surface. This assumption was confirmed by SEM analysis of the worn surface of deformed titanium: in the surface layer, we fixed a smaller number of pores and their size, acting as concentrators of crack growth. Also, a much smaller number of cracks was nucleated from such pores. It was associated with formation of a deformed surface layer after the BB. According to studies [38,39], BB of titanium alloys provides the formation of wear resistant layer with compacted structure and residual compressive stress. The last two characteristics of the layer contribute to the inhibition of the nucleation and the growth of surface micro-cracks which increases the resistance to fatigue wear.

As mentioned above, oxidative and abrasive wear are secondary wear mechanisms. Since BB (surface deformation) reduces the intensity of adhesive and fatigue wear, the oxidative and abrasive components are also less shown compared to untreated porous titanium. It was confirmed by SEM (Figures 9 and 10b) and EDX (Table 2) analyses: less oxygen on the surface (oxidative wear) and smaller dimensions (width) of the grooves (abrasive wear) were observed.

As a result of GN, the wear resistance of porous titanium was improved in comparison with untreated titanium. It can be explained by the fact that the formation of the surface compound layer, which consists of titanium nitrides  $\text{Ti}_2\text{N}$  and  $\text{TiN}$  (Figure 6), and an underlying diffusion zone change the several wear mechanisms of the studied tribo-pair

on one dominant mechanism—abrasive (Figures 9 and 10c). That is, as a result of the formation of the surface compound layer (Figure 6), which has high surface hardness (Figure 3a) and chemical inertness [27,56], the effect of the so-called ‘cold micro welding’ does not occur, which is typical for adhesive wear, but is instead levelled. The formation of a diffusion zone due to solid solution hardening of the subsurface layer [57,58] significantly reduces the probability of the formation of subsurface micro-cracks in pores (Figure 11c) and delamination in subsurface layers (Figures 9 and 11c), which is typical for the fatigue mechanism.

The dominant abrasive wear was evidenced by the results of SEM analysis of worn surfaces, where a grooved relief on the counterbody (bronze) surface (Figure 10c) was observed. The mechanism of such wear can be explained as follows: after GN, the surface roughness parameter of porous titanium increases (Figure 3b) due to the formation of a nitride layer (Figure 6). In this case, the highest places (peaks) of the surface profile correspond to titanium nitride phases. Hard nitride phases (Figure 3a), like an abrasive, cut or plow softer surface of the counterbody (Table 1), form characteristic grooved relief (Figure 10c).

The surface topography of nitrided porous titanium remains practically unchanged after friction (Figures 4 and 9c). However, according to EDX analysis (Figure 9c and Table 2), local areas of counterbody’s material were fixed on nitrided surfaces. It is obvious that during friction, the material of the counterbody is transferred to the nitrided titanium surface due to not the adhesive, but most likely the abrasive wear mechanism. Some products of micro-cutting of the bronze surface (debris) do not leave the contact area but settle (or stick) on the nitrided surface in the depressions of the microrelief or in the surface pores (Figure 9c).

Both GN and DDT of porous titanium provide the formation of a nitride layer with an underlying diffusion zone. According to XRD analysis, the intensity of nitride phases is higher for titanium after DDT than after GN, which indirectly indicates the formation of thicker surface nitride layer (Figure 6).

The wear mechanism occurring due to the formation of the surface compound layer also corresponds to the abrasive one. However, on the surface of the bronze counterbody, which was investigated in a tribo-pair with deformation–diffusion hardened porous titanium, we fixed grooves (Figure 10d), the width and depth of which were smaller than those observed on the bronze surface worked in a tribo-pair with nitrided porous titanium. The lower intensity of abrasive wear of the tribo-pair is associated not so much with the surface microhardness (since porous titanium does not lose mass and does not change the surface topography) but with the surface roughness. After the DDT, the surface quality is better (the roughness parameter  $R_a$  is lesser) than after nitriding (Figure 3b); that is, the lower surface peaks of the nitride phases (Figure 4d) deepen into the bronze phase with lower intensity and cut or plow its surface.

In summary, we can conclude that the porosity of titanium under these conditions of triboconjugation is a negative fact that needs to be leveled. The most promising method in this work is combined deformation–diffusion processing. This is explained by the fact that ball burnishing in this work ensures the closure of surface pores and, as a result, a reduction in the intensity of adhesive wear. However, this deformation treatment of the grinding wheel affects the intensity of adhesive wear, the cause of which is not only porosity, but the very nature of titanium (low hardness and thermal conductivity, chemical activity, etc.). Gas nitriding, on the contrary, makes it possible to form a chemically inert and hard nitride layer, which is not prone to adhesion. However, the formed nitride layer is thin (up to 3  $\mu\text{m}$ ), which does not allow complete coverage of the large and deep (up to 50  $\mu\text{m}$ ) surface pores. The originality and perspective of deformation–diffusion processing is that this processing allows combining the strengths and eliminating the weaknesses of traditional processing such as ball burnishing or nitriding. Therefore, this treatment can be applied to porous titanium, which works under conditions of tribo-coupling. However, it should

also be noted that such processing is annealed to the configuration of the titanium product, since preliminary ball burnishing can be used for cylindrical and simple parts.

## 5. Conclusions

In this research, the tribological properties of highly porous titanium in a tribo-pair with bronze under boundary lubrication conditions were investigated. The following conclusions were drawn:

1. It was shown that surface hardening of highly porous titanium by BB, GN, and DDT reduces the weight wear intensity and the friction coefficient of the tribo-pairs by 1.4, 3.5, 4.0 and 1.8, 2.3, 3.2 times, respectively.
2. The main wear mechanisms of highly porous titanium were adhesion and fatigue, and secondary ones were oxide and abrasive. Subsurface pores led to nucleation of micro-cracks in the subsurface layer, thereby intensifying fatigue (delamination) wear.
3. The BB, due to the closing of subsurface pores, roughness improvement and surface hardness increment, reduced adhesion and fatigue wear intensity. The GN and DDT, due to the formation of a surface compound nitride layer (TiN and Ti<sub>2</sub>N), changed the mechanism of the adhesion and fatigue wear of c.p. titanium on an abrasive one.
4. The highest wear resistance of the tribo-pair under these friction conditions was fixed for highly porous titanium after DDT.

**Author Contributions:** S.L.: conceptualization, project administration, investigation, visualization, writing—original draft preparation; I.P.: resources, methodology, supervision, writing—review and editing; J.P.: methodology, investigation, writing—review and editing; K.S.: investigation, writing—review and editing. All authors have read and agreed to the published version of the manuscript.

**Funding:** This research received no external funding.

**Institutional Review Board Statement:** Not applicable.

**Informed Consent Statement:** Not applicable.

**Data Availability Statement:** The data that support the findings of this study are available from the corresponding author upon reasonable request.

**Acknowledgments:** The authors express gratitude to Serhii Sheykin (Bakul Institute for Superhard Materials of the NAS of Ukraine), who carried on ball burnishing of the specimens and made this study possible.

**Conflicts of Interest:** The authors declare no conflict of interest.

## References

1. Froes, F.H. Powder metallurgy of titanium alloys. In *Woodhead Publishing Series in Metals and Surface Engineering, Advances in Powder Metallurgy*; Chang, I., Zhao, Y., Eds.; Woodhead Publishing: Cambridge, UK, 2013; pp. 202–240. [\[CrossRef\]](#)
2. Fang, Z.Z.; Paramore, J.D.; Sun, P.; Chandran, K.S.R.; Zhang, Y.; Xia, Y.; Cao, F.; Koopman, M.; Free, M. Powder metallurgy of titanium—Past, present, and future. *Int. Mater. Rev.* **2018**, *63*, 407–459. [\[CrossRef\]](#)
3. Childerhouse, T.; Jackson, M. Near net shape manufacture of titanium alloy components from powder and wire: A review of state-of-the-art process routes. *Metals* **2019**, *9*, 689. [\[CrossRef\]](#)
4. Ma, G.; Dong, S.; Song, Y.; Qiu, F.; Savvakina, D.; Ivasishin, O.; Cheng, T. Sustaining an excellent strength–ductility combination for Ti–6Al–4V alloy prepared from elemental powder blends. *J. Mater. Res. Technol.* **2023**, *23*, 4965–4975. [\[CrossRef\]](#)
5. Vinicius, A.R.H.; Pedro, P.C.; Carlos, A.A.C.; Jose, C.B. Production of titanium alloys for advanced aerospace systems by powder metallurgy. *Mat. Res.* **2005**, *8*, 443–446. [\[CrossRef\]](#)
6. Ma, G.; Cheng, T.; Jia, H.; Yuan, L.; Ivasishin, O.M.; Savvakina, D.G. A novel method to fabricate high strength and ductility Ti–3Al–5Mo–4.5 V alloy based on TiH<sub>2</sub> and pre-hydrogenated master alloy powders. *Mater. Des.* **2023**, *227*, 111791. [\[CrossRef\]](#)
7. Fang, Z.Z.; Sun, P. Pathways to optimize performance/cost ratio of powder metallurgy titanium—A perspective. *Key Eng. Mater.* **2012**, *520*, 15–23. [\[CrossRef\]](#)
8. Bolzoni, L.; Ruiz-Navas, E.M.; Gordo, E. Understanding the properties of low-cost iron-containing powder metallurgy titanium alloys. *Mater. Des.* **2016**, *110*, 317–323. [\[CrossRef\]](#)

9. Chen, T.; Yang, C.; Liu, Z.; Ma, H.W.; Kang, L.M.; Wang, Z.; Zhang, W.W.; Li, D.D.; Li, N.; Li, Y.Y. Revealing dehydrogenation effect and resultant densification mechanism during pressureless sintering of TiH<sub>2</sub> powder. *J. Alloys Compd.* **2021**, *873*, 159792. [[CrossRef](#)]
10. Wang, Z.; Tan, Y.; Li, N. Powder Metallurgy of Titanium Alloys: A Brief Review. *J. Alloys Compd.* **2023**, *965*, 171030. [[CrossRef](#)]
11. Naseri, R.; Mitchell, D.R.G.; Gazder, A.A.; Niessen, F.; Nancarrow, M.J.B.; Savvakina, D.G.; Pereloma, E. An investigation into the microstructural response to flexural stresses of a metastable  $\beta$ -phase Ti alloy produced by blended elemental powder metallurgy. *Adv. Eng. Mater.* **2023**, 2300350. [[CrossRef](#)]
12. Xie, F.; He, X.; Cao, S.; Mei, M.; Qu, X. Influence of pore characteristics on microstructure, mechanical properties and corrosion resistance of selective laser sintered porous Ti–Mo alloys for biomedical applications. *Electrochim. Acta* **2013**, *105*, 121–129. [[CrossRef](#)]
13. Xu, W.; Lu, X.; Zhang, B.; Liu, C.; Lv, S.; Yang, S.; Qu, X. Effects of porosity on mechanical properties and corrosion resistances of PM-fabricated porous Ti-10Mo alloy. *Metals* **2018**, *8*, 188. [[CrossRef](#)]
14. Pohreluyk, I.; Lavrysh, S.; Shliakhetka, K.; Savvakina, D.; Tkachuk, O. Influence of manufacturing parameters on microstructure evolution and corrosion resistance of powder metallurgy titanium. *JOM* **2023**, *75*, 816–824. [[CrossRef](#)]
15. Ivasishin, O.M.; Bondareva, K.A.; Bondarchuk, V.I.; Gerasimchuk, O.N.; Savvakina, D.G.; Gryaznov, B.A. Fatigue resistance of powder metallurgy Ti-6Al-4V alloy. *Strength Mater.* **2004**, *36*, 225–230. [[CrossRef](#)]
16. Romero, C.; Yang, F.; Bolzoni, L. Fatigue and fracture properties of Ti alloys from powder-based processes—A review. *Int. J. Fatigue* **2018**, *117*, 407–419. [[CrossRef](#)]
17. Guo, R.P.; Cheng, M.; Zhang, C.J.; Qiao, J.W.; Cai, C.; Wang, Q.J.; Xu, D.S.; Xu, L.; Yang, R.; Shi, Y.S.; et al. Achieving superior fatigue strength in a powder-metallurgy titanium alloy via in-situ globularization during hot isostatic pressing. *Scr. Mater.* **2023**, *228*, 115345. [[CrossRef](#)]
18. Ye, H.Z.; Li, D.Y.; Eadie, R.L. Influences of porosity on mechanical and wear performance of pseudoelastic TiNi-matrix composites. *J. Mater. Eng. Perform.* **2001**, *10*, 178–185. [[CrossRef](#)]
19. Pohreluyk, I.M.; Lavrysh, S.M.; Lukyanenko, O.H. Influence of porosity on wear resistance of sintered titanium under boundary lubrication. *J. Frict. Wear* **2021**, *42*, 461–465. [[CrossRef](#)]
20. Toptan, F.; Alves, A.C.; Pinto, A.M.P.; Ponthiaux, P. Tribocorrosion behavior of bio-functionalized highly porous titanium. *J. Mech. Behav. Biomed. Mater.* **2017**, *69*, 144–152. [[CrossRef](#)]
21. Liu, Z.; Ji, F.; Wang, M.; Zhu, T. Study on the tribological properties of porous titanium sliding against tungsten carbide YG6. *Metals* **2017**, *7*, 28. [[CrossRef](#)]
22. Salahinejad, E.; Amini, R.; Marasi, M.; Hadianfard, M.J. Microstructure and wear behavior of a porous nanocrystalline nickel-free austenitic stainless steel developed by powder metallurgy. *Mater. Des.* **2010**, *31*, 2259–2263. [[CrossRef](#)]
23. Martin, F.; García, C.; Blanco, Y. Influence of residual porosity on the dry and lubricated sliding wear of a powder metallurgy austenitic stainless steel. *Wear* **2015**, *328–329*, 1–7. [[CrossRef](#)]
24. Shibata, K.; Ishigaki, W.; Koike, T.; Umetsu, T.; Yamaguchi, T.; Hokkirigawa, K. Friction and wear behavior of stainless steel fabricated by powder bed fusion process under oil lubrication. *Tribol. Int.* **2016**, *104*, 183–190. [[CrossRef](#)]
25. Munagala, V.N.V.; Bessette, S.; Gauvin, R.; Chromik, R.R. Sliding wear of cold sprayed Ti6Al4V coatings: Effect of porosity and normal load. *Wear* **2020**, *450–451*, 203268. [[CrossRef](#)]
26. Chen, Q.; Li, D.Y.; Cook, B. Is porosity always detrimental to the wear resistance of materials?—A computational study on the effect of porosity on erosive wear of TiC/Cu composites. *Wear* **2009**, *267*, 1153–1159. [[CrossRef](#)]
27. Pohreluyk, I.M.; Fedirko, V.M.; Lavrysh, S.M. Effect of preliminary ball burnishing on wear resistance of the nitrided VT22 alloy. *J. Frict. Wear* **2017**, *38*, 221–224. [[CrossRef](#)]
28. Qu, J.; Blau, P.J.; Watkins, T.R.; Cavin, O.B.; Kulkarni, N.S. Friction and wear of titanium alloys sliding against metal, polymer, and ceramic counterfaces. *Wear* **2005**, *258*, 1348–1356. [[CrossRef](#)]
29. Redmore, E.; Li, X.; Dong, H. Tribological performance of surface engineered low-cost beta titanium alloy. *Wear* **2019**, *426–427*, 952–960. [[CrossRef](#)]
30. Chamgordani, S.A.; Miresmaeili, R.; Aliofkhaeaei, M. Improvement in tribological behavior of commercial pure titanium (CP-Ti) by surface mechanical attrition treatment (SMAT). *Tribol. Int.* **2018**, *119*, 744–752. [[CrossRef](#)]
31. Bansal, D.G.; Eryilmaz, O.L.; Blau, P.J. Surface engineering to improve the durability and lubricity of Ti-6Al-4V alloy. *Wear* **2011**, *271*, 2006–2015. [[CrossRef](#)]
32. Nazarenko, P.V.; Polishchuk, I.E.; Molyar, A.G.; Ostranitsa, A.E. Tribotechnical properties of coatings on titanium alloys. *Mater. Sci.* **1998**, *34*, 203–210. [[CrossRef](#)]
33. Klint, R.V.; Owens, R.S. Lubrication of diffusion-beryllided titanium. *ASLE Trans.* **1962**, *5*, 32–38. [[CrossRef](#)]
34. Kukareko, V.A.; Belotserkovsky, M.A.; Grigorchik, A.N.; Sosnovskiy, A.V. Structure and tribological properties of a Ti–TiN coating obtained by hypersonic metallization. *J. Frict. Wear* **2022**, *43*, 300–304. [[CrossRef](#)]
35. Quan, X.; Xie, H.; Xu, X.; Tang, J. Study on the enhanced tribological performance for titanium alloys by PEG oil/Zn-nanoparticles. *Mater. Res. Express* **2020**, *7*, 126502. [[CrossRef](#)]
36. Blau, P.J.; Cooley, K.M.; Bansal, D.; Smid, I.; Eden, T.J.; Neshastehriz, M.; Potter, J.K.; Segall, A.E. Spectrum loading effects on the running-in of lubricated bronze and surface-treated titanium against alloy steel. *Wear* **2013**, *302*, 1064–1072. [[CrossRef](#)]

37. Avcu, Y.Y.; Iakovakis, E.; Guney, M.; Çalım, E.; Özkılınc, A.; Abakay, E.; Sönmez, F.; Koç, F.G.; Yamaoğlu, R.; Cengiz, A.; et al. Surface and tribological properties of powder metallurgical Cp-Ti titanium alloy modified by shot peening. *Coatings* **2023**, *13*, 89. [[CrossRef](#)]
38. Revankar, G.D.; Shetty, R.; Rao, S.S.; Gaitonde, V.N. Wear resistance enhancement of titanium alloy (Ti-6Al-4V) by ball burnishing process. *J. Mater. Res. Technol.* **2017**, *6*, 13–32. [[CrossRef](#)]
39. Pohrelyuk, I.M.; Lavrys, S.M. Load influence at rolling on structure and wear resistance of a titanium alloy VT22. *Metallofiz. Noveishie Tekhnol.* **2016**, *38*, 783–793. [[CrossRef](#)]
40. Kato, H.; Ueki, H.; Yamamoto, K.; Uasunaga, K. Wear resistance improvement by nanostructured surface layer produced by burnishing. *Mater. Sci. Forum* **2018**, *917*, 231–235. [[CrossRef](#)]
41. Dekhtyar, A.I.; Mordiyuk, B.N.; Savvakina, D.G.; Bondarchuk, V.I.; Moiseeva, I.V.; Khripta, N.I. Enhanced fatigue behavior of powder metallurgy Ti-6Al-4V alloy by applying ultrasonic impact treatment. *Mater. Sci. Eng. A* **2015**, *641*, 348–359. [[CrossRef](#)]
42. Balla, K.; Bose, S.; Bandyopadhyay, A. Understanding compressive deformation in porous titanium. *Philos. Mag.* **2010**, *90*, 3081–3094. [[CrossRef](#)]
43. Lavrys, S.; Pohrelyuk, I.; Tkachuk, O.; Padgurskas, J.; Trush, V.; Proskurnyak, R. Comparison of Friction Behaviour of Titanium Grade 2 after Non-Contact Boriding in Oxygen-Containing Medium with Gas Nitriding. *Coatings* **2023**, *13*, 282. [[CrossRef](#)]
44. Dai, Y.; Jiang, X.; Ou, M.; Li, K.; Xiang, Q.; Yang, F.; Liu, J. Tribocorrosion Behaviour of a Ti-25Nb-3Zr-2Sn-3Mo Alloys Induction Nitride Layer in a Simulated Body Fluid Solution. *Coatings* **2023**, *13*, 231. [[CrossRef](#)]
45. Pohrelyuk, I.M.; Fedirko, V.M.; Lavrys, S.M.; Kravchyshyn, T.M. Regularities of thermal diffusion saturation with nitrogen combined with standard heat treatment of VT22 titanium alloy. *Mater. Sci.* **2017**, *52*, 841–847. [[CrossRef](#)]
46. Bakdemir, S.A.; Özkan, D.; Türküz, C.; Salman, S. Wear performance under dry and lubricated conditions of duplex treatment TiN/TiCrN coatings deposited with different numbers of CrN interlayers on steel substrates. *Wear* **2023**, *526–527*, 204931. [[CrossRef](#)]
47. Łepicka, M.; Grądzka-Dahlke, M.; Pieniak, D.; Pasierbiewicz, K.; Kryńska, K.; Niewczas, A. Tribological performance of titanium nitride coatings: A comparative study on TiN-coated stainless steel and titanium alloy. *Wear* **2019**, *422–423*, 68–80. [[CrossRef](#)]
48. Wen, K.; Zhang, C.; Gao, Y. Influence of gas pressure on the low-temperature plasma nitriding of surface-nanocrystallined TC4 titanium alloy. *Surf. Coat. Technol.* **2022**, *436*, 128327. [[CrossRef](#)]
49. She, D.; Yue, W.; Kang, J.; Huang, F.; Wang, C.; Shen, J. Vacuum tribological properties of titanium enhanced via ultrasonic surface rolling processing pre-treatment and plasma nitriding. *Tribol. Trans.* **2018**, *61*, 612–620. [[CrossRef](#)]
50. Toboła, D.; Morgiel, J.; Maj, Ł. TEM analysis of surface layer of Ti-6Al-4V ELI alloy after slide burnishing and low-temperature GN. *Appl. Surf. Sci.* **2020**, *515*, 145942. [[CrossRef](#)]
51. Lijesh, K.P.; Khonsari, M.M. On the onset of steady state during transient adhesive wear. *Tribol. Int.* **2019**, *130*, 378–386. [[CrossRef](#)]
52. Su, J.; Xie, H.; Tan, C.; Xu, Z.; Liu, J.; Jiang, F.; Tang, J.; Fu, D.; Zhang, H.; Teng, J. Microstructural characteristics and tribological behavior of an additively manufactured Ti-6Al-4V alloy under direct aging and solution-aging treatments. *Tribol. Int.* **2022**, *175*, 107763. [[CrossRef](#)]
53. Abdelbary, A.; Chang, L. Tribology of metals and alloys. In *Principles of Engineering Tribology*; Abdelbary, A., Chang, L., Eds.; Academic Press: Cambridge, MA, USA, 2023; pp. 207–234. [[CrossRef](#)]
54. Michael, J.R.; Kotula, P.G.; Prasad, S.V. Electron microscopy and microanalysis for wear surface characterization. In *Advanced Analytical Methods in Tribology*; Dienwiebel, M., De Barros Bouchet, M.I., Eds.; Springer: Berlin/Heidelberg, Germany, 2018; pp. 3–28. [[CrossRef](#)]
55. Tabrizi, A.T.; Aghajani, H.; Saghafian, H.; Laleh, F.F. Correction of Archard equation for wear behavior of modified pure titanium. *Tribol. Int.* **2021**, *155*, 20–27. [[CrossRef](#)]
56. Skvortsova, S.; Spektor, V.; Pozhoga, O.; Gvozdeva, O. The effect of the surface structure of titanium alloy medical screws on their wear resistance. *MATEC Web Conf.* **2019**, *298*, 00067. [[CrossRef](#)]
57. Fedirko, V.N.; Luk'yanenko, A.G.; Trush, V.S. Solid-solution hardening of the surface layer of titanium alloys. *Part 1. Effect on mechanical properties, Met. Sci. Heat Treat.* **2014**, *56*, 368–373. [[CrossRef](#)]
58. Shen, H.; Wang, L. Tribological properties of Ti-N compound layer formed on Ti6Al4V by HCD assisted plasma nitriding. *Mater. Today Commun.* **2023**, *36*, 106652. [[CrossRef](#)]

**Disclaimer/Publisher's Note:** The statements, opinions and data contained in all publications are solely those of the individual author(s) and contributor(s) and not of MDPI and/or the editor(s). MDPI and/or the editor(s) disclaim responsibility for any injury to people or property resulting from any ideas, methods, instructions or products referred to in the content.